Progress In Electromagnetics Research M, Vol. 35, 121–131, 2014

Survey of Temporal Basis Functions for Transient Scattering by Conducting Cylinders Using TD-EFIE Formulation-TE Case

Athar Azari*, Zaker H. Firouzeh, and Abolghasem Zeidaabadi-Nezhad

Abstract—In this paper, different causal sub-domain temporal basis functions are investigated to make the explicit marching-on-in time schemes converge and stable for solving two dimensional time domain EFIE. PEC cylinders with arbitrary cross section are illuminated by a TE-polarized Gaussian plane wave. Two different approximations are used for calculation of the singular elements of the impedance matrix analytically. In the Time Domain Method of Moment (TD-MoM) formulation of the Electric Field Integral Equation (EFIE) of the problem, the free-space two-dimensional Green's function and triangular spatial basis function are used. By employing Galerkin's method in spatial domain and point matching in time domain, all time convolution integrals and self-terms are evaluated analytically to increase the accuracy and stability of the proposed technique. The stability and efficiency of the new technique are confirmed by comparison with literature.

1. INTRODUCTION

Methods based on time domain integral equations (TDIEs) have been widely used to analyze scattering from conducting and dielectric surfaces and also characterizing transient radiation from antennas [1]. The advantages of TDIE methods in regards to finite difference time domain (FDTD) technique are the solution of fewer unknowns due to using surface discretization and exclusion of absorbing boundary conditions (ABCs) for open-region problems [2].

In recent years, well-known integral equation (IE) formulation having either the electric field or the magnetic field as unknown (EFIE or MFIE, respectively) is used to compute the transient electromagnetic scattering by a perfectly conducting cylinder and solved by the time-domain method of moments (TD-MoM). The free-space two-dimensional Green's function is firstly used by Bennett and Weeks [3] to calculate the transient currents on conducting cylinders by a numerical solution of the time-domain magnetic field integral equation (TD-MFIE). The scattered field is obtained by the so-called marching-on-in-time method (MOT) at each space-time point. In [4], an implicit solution approach was applied to transverse electric (TE) incidence onto two-dimensional conducting cylinders, for both EFIE and MFIE formulations. Although the solution technique was simple, accurate and stable, two main drawbacks were observed, i.e., late-time instability and high computational complexity. The unintended latetime growing oscillations are originated at the system discretization step in the conversion of the integral equation to a discrete time-space model [5]. Many techniques have been developed to solve the late-time instability [6, 7]. In addition, the TDIE formulations suffer from great difficulties for electrically large objects, due to the need of using fast algorithms to solve TDIEs. In the past decades, many fast algorithms such as time domain fast dipole method (TD-FDM) [8], multilevel time domain fast dipole method [9] and the hybrid of TDIE and time domain physical optics (TDPO) methods [10] have been introduced to reduce the memory requirement and computational complexity of the MOT scheme. A wise solution to significantly enhance the extent of the stable region, reduce numerical errors

Received 5 February 2014, Accepted 16 March 2014, Scheduled 20 March 2014

* Corresponding author: Athar Azari (a.azari@ec.iut.ac.ir).

The authors are with the Department of Electrical and Computer Engineering, Isfahan University of Technology, Isfahan 84156, Iran.

and increase the efficiency is to use analytical time derivatives and time convolution integrals arising in the TDIEs [11, 12]. One effective approach to improve the stability and convergence of the MOT scheme is to use proper temporal basis functions (TBFs) for interpolation between discrete time samples [13].

The purpose of this paper is to investigate the effect of various temporal basis functions on the convergence and late-time stability of TD-MoMs for solving the time-domain electric field integral equation (TD-EFIE) of a conducting cylinder illuminated by transverse electric (TE) incident Gaussian plane waves. The cylinder is presumed to have an arbitrary cross section and to be infinitely long. The two-dimensional time-domain Green's function is used to develop the TD-EFIE in which the time convolution integral is calculated analytically to increase the accuracy and stability. Moreover, the logarithmic singularity of self-terms is dealt with analytically. Five different TBFs such as rectangular, triangular, quadratic Lagrange, cubic Lagrange and shifted quadratic B-Spline are used to solve the TD-EFIE formulation. Then, the final matrix equation is solved by means of an explicit MOT procedure which leads to the space-time current distribution on the conducting two-dimensional cylinder.

The paper is organized as follows. In the next section, the problem is formulated, and its related TD-EFIE is solved by a TD-MoM scheme. In addition, five different temporal basis functions (TBFs) are presented to develop the TD-MoM solution. Section 3 describes two approximate formulations to calculate self-terms analytically. Numerical results are presented in Section 4, including a comparison with results from literature. This section also discusses the efficiency and convergence properties of the proposed algorithm. Finally, conclusions are given.

2. FORMULATION

Consider an infinite perfectly electric conducting (PEC) cylinder with arbitrary cross section that resides parallel to z-axis in free space (permittivity ε_0, permeability μ_0). As shown in Figure 1, C denotes the circumference of the cross section of the cylinder. $\mathbf{a}_n$ represents an outward-directed unit vector normal to the contour C in each point. The tangential vector $\mathbf{a}_\tau$ is then obtained by $\mathbf{a}_\tau = \mathbf{a}_z \times \mathbf{a}_n$. The conducting cylinder is illuminated by a TE-polarized plane wave. Therefore, the incident magnetic field is parallel to z-axis. The incident electric field $\mathbf{E}^{inc}$ induces a continuous surface current $\mathbf{J}$ in the transverse direction of the cylinder axis, which produces the scattered field. By enforcing the boundary condition for the electric field on the cylinder surface the EFIE equation is obtained as:

$$\left[\frac{\partial \mathbf{A}}{\partial t} + \nabla\Phi\right]_{\tan} = \left[\mathbf{E}^{inc}\right]_{\tan} \tag{1}$$

where

$$\mathbf{A}(\boldsymbol{\rho}, t) = \mu_0 \int_C \mathbf{J}(\boldsymbol{\rho}', t) * G(\boldsymbol{\rho}, t; \boldsymbol{\rho}')\, dc' \tag{2}$$

$$\Phi(\boldsymbol{\rho}, t) = \frac{1}{\varepsilon_0} \int_C \boldsymbol{\rho}_s(\boldsymbol{\rho}', t) * G(\boldsymbol{\rho}, t; \boldsymbol{\rho}')\, dc' \tag{3}$$

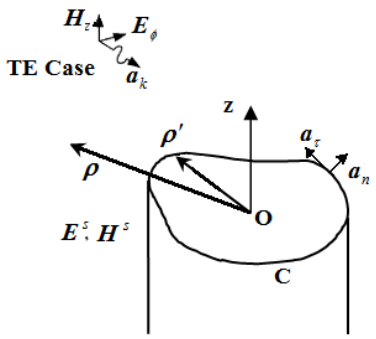

Figure 1. A conducting cylinder illuminated by a TM transient pulse.

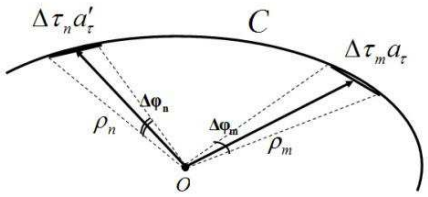

Figure 2. The cylinder circumference is subdivided into segments.

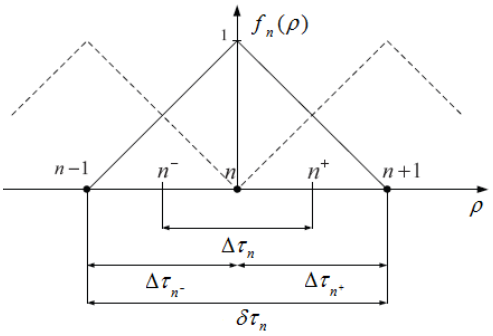

Figure 3. Triangular spatial basis function.

$$G(\boldsymbol{\rho}, t; \boldsymbol{\rho}') = \frac{u(t - R/c_0)}{2\pi\sqrt{t^2 - (R/c_0)^2}} \tag{4a}$$

$$R = \left|\boldsymbol{\rho} - \boldsymbol{\rho}'\right| \tag{4b}$$

$G(\boldsymbol{\rho}, t; \boldsymbol{\rho}')$ is the two-dimensional Green's function in time domain. R is the distance between the observation point $\boldsymbol{\rho}$ and the source point $\boldsymbol{\rho}'$. The surface electric charge density is denoted by $\boldsymbol{\rho}_s$. The time-domain convolution is denoted by $*$, and $u(t)$ is the Heaviside step function. c_0 is the speed of light in free space.

The TD-EFIE can be solved numerically by discretizing the surface current density in both space and time with N_s spatial basis functions and N_t temporal basis functions:

$$\mathbf{J}(\boldsymbol{\rho}, t) = \mathbf{a}_\tau \sum_{n=1}^{N_s} \sum_{i=1}^{N_t} I_n^i f_n(\boldsymbol{\rho})\, g_i(t) \tag{5}$$

where I_n^i is the unknown real coefficient at a time t_i for the nth segment. $f_m(\boldsymbol{\rho})$ and $g_i(t)$ are the spatial and temporal basis functions respectively.

Let the cylinder circumference C be subdivided into segments with length $\Delta\tau_m$, as shown in Figure 2. Note that all the field quantities are invariant with respect to the z axis because the cylinder is infinite along the axis. Moreover, the current flow is continuous along the contour C. It is necessary the spatial basis functions are zero at the boundary points of the integration interval due to using the proposed formulation. In addition, the expansion functions around the contour can extend across any bend or edge. Therefore, the spatial basis functions, $f_n(\boldsymbol{\rho})$, used here are triangular as shown in Figure 3.

The temporal expansion functions should have the analytical time convolution integral. In addition, these basis functions should be casual to simply use in the MOT algorithm. Here the rectangular, triangular, quadratic Lagrange, cubic Lagrange and shifted quadratic B-Spline TBFs are used and defined as (6a) to (6e) relations respectively [5]. In the special case of quadratic B-Spline, the function is shifted by $\Delta t/2$ in time to make the function causal. These functions are plotted in Figure 4.

$$g_0(t) = \begin{cases} 1 & |t| < \Delta t/2 \\ 0 & \text{elsewhere} \end{cases} \tag{6a}$$

$$g_0(t) = \begin{cases} 1 - t/\Delta t & |t| \le \Delta t \\ 0 & \text{elsewhere} \end{cases} \tag{6b}$$

$$g_0(t) = \begin{cases} 1 \pm \frac{3}{2}\left(\frac{t}{\Delta t}\right) + \frac{1}{2}\left(\frac{t}{\Delta t}\right)^2 & +: -\Delta t \le t \le 0,\ -: \Delta t \le t \le 2\Delta t \\ 1 - \left(\frac{t}{\Delta t}\right)^2 & 0 \le t \le \Delta t \\ 0 & \text{elsewhere} \end{cases} \tag{6c}$$

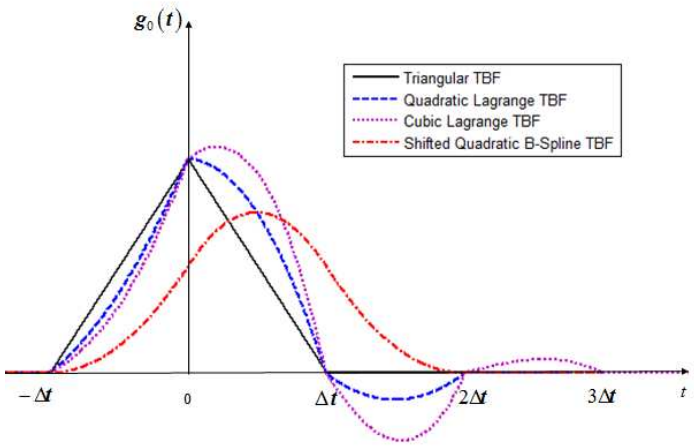

Figure 4. The various temporal basis functions.

$$g_0(t) = \begin{cases} 1+\frac{11}{6}\left(\frac{t}{\Delta t}\right)+\left(\frac{t}{\Delta t}\right)^2+\frac{1}{6}\left(\frac{t}{\Delta t}\right)^3 & -\Delta t \le t \le 0 \\ 1+\frac{1}{2}\left(\frac{t}{\Delta t}\right)-\left(\frac{t}{\Delta t}\right)^2-\frac{1}{2}\left(\frac{t}{\Delta t}\right)^3 & 0 \le t \le \Delta t \\ 1-\frac{1}{2}\left(\frac{t}{\Delta t}\right)-\left(\frac{t}{\Delta t}\right)^2+\frac{1}{2}\left(\frac{t}{\Delta t}\right)^3 & \Delta t \le t \le 2\Delta t \\ 1-\frac{11}{6}\left(\frac{t}{\Delta t}\right)+\left(\frac{t}{\Delta t}\right)^2-\frac{1}{6}\left(\frac{t}{\Delta t}\right)^3 & 2\Delta t \le t \le 3\Delta t \\ 0 & \text{elsewhere} \end{cases} \tag{6d}$$

$$g_0(t) = \begin{cases} \frac{1}{2}\left(\frac{t}{\Delta t}\right)^2+\left(\frac{t}{\Delta t}\right)+\frac{1}{2} & -1 \le \frac{t}{\Delta t} < 0 \\ -\left(\frac{t}{\Delta t}\right)^2+\left(\frac{t}{\Delta t}\right)+\frac{1}{2} & 0 \le \frac{t}{\Delta t} < 1 \\ \frac{1}{2}\left(\frac{t}{\Delta t}\right)^2-2\left(\frac{t}{\Delta t}\right)+2 & 1 \le \frac{t}{\Delta t} < 2 \\ 0 & \text{elsewhere} \end{cases} \tag{6e}$$

Furthermore, the temporal basis function $g_i(t)$ at time $i\Delta t$ is related to $g_0(t)$ by

$$g_i(t) = g_0(t - i\cdot\Delta t), \quad i = 0, 1, \ldots, N_t \tag{7}$$

where Δt is the time step of the analysis.

Substituting (5) in (2) and (3), employing $f_m(\boldsymbol{\rho})$ as testing functions and point matching at the $t_k = k\cdot\Delta t$ in space and time, respectively, and the inner product defined in (8) for TD-EFIE (1), the TD-MoM formulation is obtained as follows.

$$\langle \mathbf{a}, \mathbf{b}\rangle = \int_C \mathbf{a}\cdot\mathbf{b}dC' \tag{8}$$

$$\left\langle f_m\mathbf{a}_\tau, \frac{\partial\mathbf{A}}{\partial t}\right\rangle\Big|_{t=t_k} + \langle f_m\mathbf{a}_\tau, \nabla\Phi\rangle|_{t=t_k} = \left\langle f_m\mathbf{a}_\tau, \mathbf{E}^{inc}\right\rangle\Big|_{t=t_k} \tag{9}$$

$$\langle f_m\mathbf{a}_\tau, \mathbf{E}^{inc}\rangle\big|_{t=t_k} = \mathbf{E}^{inc}(\boldsymbol{\rho}_m, k\Delta t)\cdot\Delta\tau_m\mathbf{a}_\tau \tag{10}$$

$$\left\langle f_m\mathbf{a}_\tau, \frac{\partial\mathbf{A}}{\partial t}\right\rangle\Big|_{t=t_k} = \mu_0\sum_{n=1}^{N_s}\sum_{i=1}^{N_t} I_n^i\Delta\tau_m\Delta\tau_n\zeta_{mn}(t_{k-i}) \tag{11}$$

$$\langle f_m\mathbf{a}_\tau, \nabla\Phi\rangle|_{t=t_k} = \mu_0c_0^2\sum_{n=1}^{N_s}\sum_{i=1}^{N_t} I_n^i\left(\zeta_{m^+n^+}(t_{k-i}) - \zeta_{m^+n^-}(t_{k-i}) - \zeta_{m^-n^+}(t_{k-i}) + \zeta_{m^-n^-}(t_{k-i})\right) \tag{12}$$

where

$$\zeta_{mn}(t_{k-i}) = \frac{1}{\Delta\tau_m\Delta\tau_n}\int_{\Delta\tau_m}\int_{\Delta\tau_n}\mathbf{a}_\tau\cdot\mathbf{a}_{\tau'}\left(\frac{\partial}{\partial t}g_0(t) * G\left(\boldsymbol{\rho}, t; \boldsymbol{\rho}'\right)\right)\Big|_{t=t_{k-i}} d\tau' d\tau \tag{13}$$

$$\zeta_{m^{\pm}n^{\pm}}(t_{k-i}) = \frac{1}{\Delta\tau_{m^{\pm}}\Delta\tau_{n^{\pm}}}\int_{\Delta\tau_{m^{\pm}}}\int_{\Delta\tau_{n^{\pm}}}\left(G_0(t) * G\left(\boldsymbol{\rho}, t; \boldsymbol{\rho}'\right)\right)\big|_{t=t_{k-i}}\, d\tau' d\tau \tag{14}$$

$$G_i(t) = \int_{-\infty}^{t} g_i(t')dt' \tag{15}$$

Equation (12) is derived by applying integration by parts with respect to τ and making use of the fact that the spatial basis functions $f_m(\boldsymbol{\rho})$ are zero at the boundary points of the integration interval $\delta\tau_m$ as shown in Figure 3. Moreover, the derivative of $f_n(\boldsymbol{\rho}')$ generates two rectangular pulses with positive and negative amplitudes centered at n^- and n^+, respectively.

It is worth mentioning that the triangular basis functions in (10) and (11) can be replaced by rectangular basis functions without noticeably affecting the accuracy of the final result [14]. Equations (9)–(15) form the following matrix equations from which the current distribution on the infinite conducting cylinder can be obtained

$$\sum_{i=1}^{N_t}\left[\Phi^{k-i}\right]_{N_s\times N_s}\cdot\left[I^i\right]_{N_s\times 1} = \left[V^k\right]_{N_s\times 1}, \quad k = 1, 2, \ldots, N_t \tag{16}$$

$$\varphi_{mn}^{(k-i)} = \mu_0\Delta\tau_m\Delta\tau_n\zeta_{mn}(t_{k-i}) + \mu_0 c_0^2\left(\zeta_{m^+n^+}(t_{k-i}) - \zeta_{m^+n^-}(t_{k-i}) - \zeta_{m^-n^+}(t_{k-i}) + \zeta_{m^-n^-}(t_{k-i})\right) \tag{17}$$

$$\mathbf{v}_m^k = \mathbf{E}^{inc}(\boldsymbol{\rho}_m, k\Delta t)\cdot\Delta\tau_m\mathbf{a}_\tau \tag{18}$$

$[V^k]$ and $[I^i]$ are column vectors representing the incident field at time $k\Delta t$, and the spatial current distribution on the segments at time $i\Delta t$, respectively. The matrix $[\Phi^{k-i}]$ relates the spatial current distribution on the segments at time $i\Delta t$ to the scattered electric field component tangential to the segments at time $k\Delta t$.

According to the temporal basis functions and using causality, (16) is reduced to

$$\left[I^1\right] = \left[\Phi^0\right]^{-1}\cdot\left[V^1\right], \quad \text{for } k = 1 \tag{19}$$

$$\left[I^k\right] = \left[\Phi^0\right]^{-1}\cdot\left(\left[V^k\right] - \sum_{i=1}^{k-1}\left[\Phi^{k-i}\right]\cdot\left[I^i\right]\right), \quad \text{for } k \geq 2 \tag{20}$$

Note that the $[\Phi^0]$ matrix contains vector potential terms, and the $[V^k]$ vector represents the incident field at time t_k which are known. The $[\Phi^0]$ matrix is a near diagonal matrix, in which the elements $\varphi_{m,m}^0$ are related to self-coupling and $\varphi_{m,(m+1)}^0$ and $\varphi_{(m+1),m}^0$ are related to the near coupling. The numerical procedure starts at $k = 2$, assuming the current to be zero at $k = 1$, and then marches on in time for $k = 3, 4, 5, \ldots, N_t$. This form is called the explicit marching-on in time formulation [15]. The time convolutions in (13) and (14) are analytically calculated for the different TBFs using (6a)–(6e). For instance, the time convolutions using the triangular TBF (6b) has been given in Appendix A.

The spatial integral for far segments can be approximated by the product of the segment length $\Delta\tau_m$ and the integrand in which R is replaced by $R_{m,n}$ as follows.

$$R_{m,n} = \left|\boldsymbol{\rho}_m - \boldsymbol{\rho}_n\right|, \quad m \neq n. \tag{21}$$

For various temporal basis functions when calculating the elements $\varphi_{m,m}^0$, $\varphi_{m,(m+1)}^0$ and $\varphi_{(m+1),m}^0$, the integrands in (13) and (14) may have logarithmic singularity which should be calculated analytically. The singularity extraction is used to overcome this problem as described in the next section.

3. THE SINGULARITY EXTRACTION TECHNIQUE

As mentioned in the previous section, the integrands in (13) and (14) have logarithmic singularity which can be extracted analytically. In this scheme, the singular parts are integrated with first- and second-order approximations as follows.

The main singular part of the mentioned integral when $t = 0$ and $m = n$ is given in (22).

$$\int_{\Delta\ell}\int_{\Delta\ell}\ln(R)\, d\ell\, d\ell' \tag{22}$$

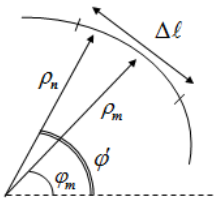

Figure 5. The self term part ($\Delta l = \Delta\tau_m$).

Referring to Figure 5 in the first-order approximation, the observation point (ρ_m, φ_m) is located at the middle of segment $\Delta\tau_m$, and the source point (ρ_m, φ') is varied over it.

The distance between source and observation points, R, is given as:

$$R = \left|\rho - \rho'\right| = 2\rho_m \sin\left(\frac{\varphi_m - \varphi'}{2}\right) \tag{23}$$

By replacing R in (22) with (23) and using the approximation of $\sin(x) \approx x$ for small arguments, the first-order approximation of the singular part can be obtained as

$$\int_{\Delta\ell}\int_{\Delta\ell} \ln|R|\; d\ell d\ell' \;=\; \Delta\ell^2\left[\ln\left(\Delta\ell/2\right) - 1\right] \tag{24}$$

In the second-order approximation, the source point (ρ_m, φ') and the observation point (ρ_m, φ) are varied over segment $\Delta\tau_m$. Then, by replacing R in (22) with (23), and expanding with 603.1 of [16] and using 610 of [16], the second-order approximation of the singular part is given as:

$$\int_{\Delta\ell}\int_{\Delta\ell} \ln|R|\; d\ell d\ell' \;=\; \Delta\ell^2\left[\ln\left(\Delta\ell/2\right) - 3/2\right] \tag{25}$$

For instance, the first- and second-order approximations to extract logarithmic singularity from self-terms using the triangular TBF (6b) has been given in Appendix B.

It is assumed that $\Delta t < R_{\min}/c_0$ due to providing a stable procedure based on the causality principle.

4. NUMERICAL RESULTS

This technique has been used to simulate different two-dimensional (2D) structures such as a straight strip, a 90° sharp bend strip, circular and square cylinders. In this section, for instance two PEC infinite cylinders are posed to demonstrate how the various temporal interpolators can provide late time stability and convergence of the solution of the transient scattering from infinitely long conducting cylinders. The numerical results of the proposed technique are obtained using five various causal TBFs viz. rectangular, triangular, quadratic Lagrange, cubic Lagrange and shifted quadratic B-Spline functions. The cylinders are illuminated by a TE Gaussian plane wave. The results obtained by the proposed technique for the straight strip are compared with those computed by using the three-dimensional (3D) Green's function of free space in [17]. Chapter 3 in [17], in fact, solves the EFIE for 2D scattering with TE incident polarizations using 3D Green's function by zero-order spatial discretization approach. In addition, the integration is carried out analytically only for self-terms and one-point integration is used for the evaluation of the rest matrix entries. In addition, the rectangular temporal basis function and the triangular spatial basis function are used. In addition, for closed smooth surfaces the proposed technique is compared with the results obtained by [3] using 2D Green's function of free space. However, the temporal differentials and convolutions of [3] have been obtained numerically. According to [6], a stable numerical result can be obtained based on Courant's stability condition, i.e., $\Delta t \leq R_{\min}/c_0\sqrt{2}$. In this work, it is used $\Delta t < R_{\min}/c_0$ — the causality principle based on numerical experience. Because all time convolutions, integrals and differentials are calculated analytically; the numerical errors are considerably decreased and the extent of stable region is enhanced favorably [18].

First, consider a straight strip of 0.5 m width centered at the origin and along the y-axis. The strip is subdivided into 10 uniform segments. The structure is illuminated by a Gaussian plane wave, given by

$$\mathbf{H}^{inc}(\boldsymbol{\rho}, t) = \mathbf{a}_z H_0 \frac{4}{T\sqrt{\pi}} e^{-\gamma^2}$$
$$\gamma = \frac{4}{T}\left(c_0 t - c_0 t_0 - \boldsymbol{\rho} \cdot \mathbf{a}_k\right) \tag{26}$$

with $H_0 = 1.0\,\mathrm{A/m}$, $\mathbf{a}_k = -\mathbf{a}_\rho$, $T = 4\,\mathrm{LM}$, and $t_0 = 6\,\mathrm{LM}$ shown in Figure 6. Note that 1 light meter (LM) is defined as the unit of time. It is the time that it takes for the electromagnetic wave to travel 1 m distance in free space. The current induced at the center of the straight strip by employing different TBFs using 1st- and 2nd-order approximations are compared in Figure 7 and Figure 8, respectively. The agreements are good in early time. The simulations are continued to study late-time behavior of the response. It is observed that the proposed technique using rectangular, triangular and cubic Lagrange TBFs and employing 2nd-order approximation extend the stable region extremely.

Next, a circular cylinder with a 1 m radius is considered. The scatterer is illuminated by the Gaussian plane wave (26) with $H_0 = 1/120\pi\,\mathrm{A/m}$, $\mathbf{a}_k = -\mathbf{a}_\rho$, $T = 2$, and $t_0 = 3\,\mathrm{LM}$ since its frequency spectrum includes a few of internal resonance frequencies of the cylinder. The circumference is uniformly subdivided into 88 segments. As shown in Figure 9 and Figure 10 although agreement is well in early time, there are some oscillations because of internal resonances. Here it is observed that by employing

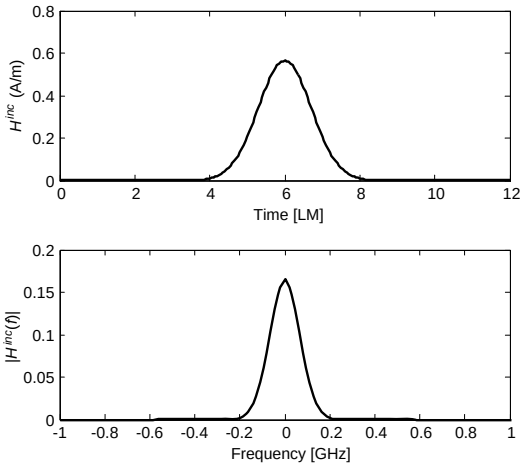

Figure 6. The Gaussian pulse of the incident field.

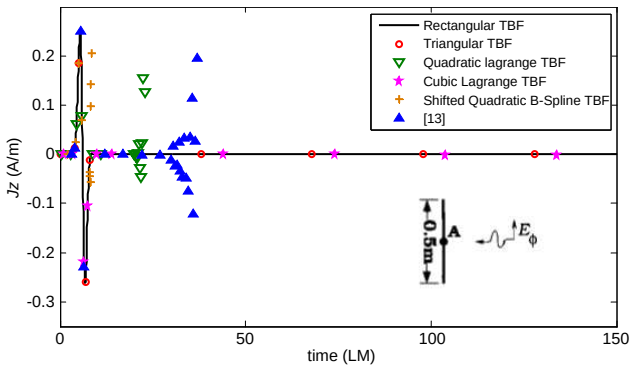

Figure 7. Comparison of transient current response at the center of the straight strip using the first-order approximation.

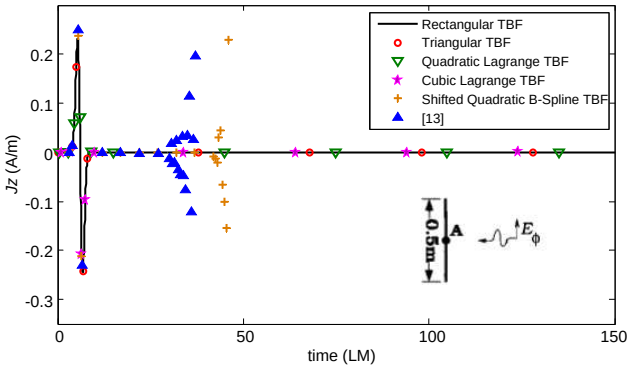

Figure 8. Comparison of transient current response at the center of the straight strip using the second-order approximation.

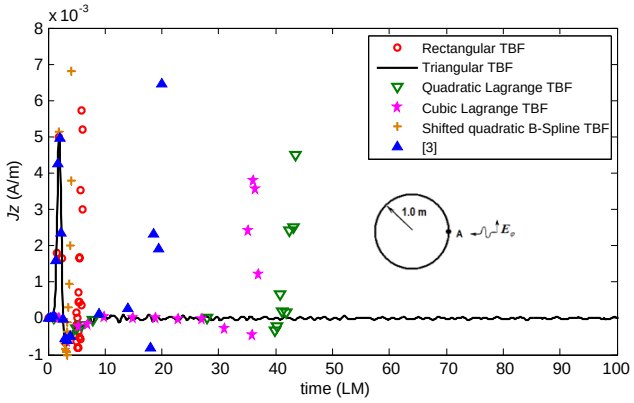

Figure 9. Comparison of transient current response at the $\varphi = 0$ of the circular cylinder with $r = 1\,\mathrm{m}$ using the first-order approximation.

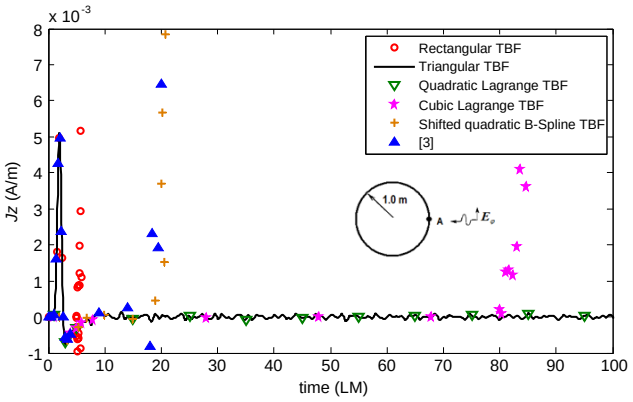

Figure 10. Comparison of transient current response at the $\varphi = 0$ of the circular cylinder with $r = 1\,\mathrm{m}$ using the second-order approximation.

1st-order approximation, only for triangular interpolator the response remains stable. However by employing the 2nd-order approximation and triangular, quadratic Lagrange and cubic Lagrange TBFs the stability region is improved. In the case of quadratic Lagrange TBF, the first-order approximation of the integrator with Courant's stability condition is not stable; however, the TD-MoM scheme is late-time stable using the second order approximation of the integrator. The augmented exponential growth in the late-time regime of the solution is principally originated at the system discretization stage, namely in the conversion of the integral equation to a discrete time–space model [5]. When higher-order approximation of the integrator is used for the self-terms there is not observed any late-time instability.

In the case of shifted quadratic B-Spline TBF although the function is smother than the same order quadratic Lagrange function, the stable region is not extended enough. Because the quadratic B-Spline function is shifted in time to make the function causal, the peak value is also shifted from zero and causes the interpolation error added to computational and discretization errors. So the instability is occurred earlier than expected. In addition, the reduction of the time step size does not influence on the stability of the solution.

Since the time domain results of the proposed technique were obtained with $\Delta t \leq R_{\min}/c_0$ the computation time is much less than the techniques of [3, 17] as shown in Table 1 and Table 2. This is because all integrals involved in (13) and (14) are calculated in the closed forms. In addition, employing continuous TBFs to evaluate analytically the time derivatives of the TDIE decreases numerical errors considerably and enhances the extent of stable region acceptably [18]. Also the late-time stability is increased by proposed technique compare to [3, 17].

The computer used in this comparison has an AMD Phenom 8650 Triple-core Processor and 2 GB of RAM. The new technique is considerably faster and more efficient as shown in Table 1 and Table 2.

Table 1. Comparison of the computation times of employing various TBFs for straight strip with $\Delta\tau = 0.05\,\mathrm{m}$ for simulation time until 15 LM.

Temporal basis function	Time step Δt (LM)	1st-order approximation (Sec.)	2nd-order approximation (Sec.)	[17] Rectangular TBF
Rectangular	0.033	1.54	2.06	$\Delta t = 0.034\,\mathrm{LM}$ 110 Sec.
Triangular	0.05	1.82	1.84	
Quadratic Lagrange	0.045	3.10	3.07	
Cubic Lagrange	0.038	5.68	5.69	
Shifted Quadratic B-Spline	0.043	2.87	2.82	

Table 2. Comparison of the computation times of employing various TBFs for circular cylinder with $\Delta\tau = 0.0714\,\mathrm{m}$ for simulation time until 15 LM.

Temporal basis function	Time step Δt (LM)	1st-order approximation (Sec.)	2nd-order approximation (Sec.)	[3] Rectangular TBF
Rectangular	0.045	$*$	$*$	$\Delta t = 0.045\,\mathrm{LM}$ 58.8 Sec.
Triangular	0.072	75.2	75.91	
Quadratic Lagrange	0.064	129.1	130.9	
Cubic Lagrange	0.052	283.1	283.5	
Shifted Quadratic B-Spline	0.065	$*$	126.1	

$*$. The response is divergerd before 15 LM.

5. CONCLUSION

In this paper, the effect of various temporal basis functions (TBFs) is investigated in TD-MoM approach to solve the TD-EFIE formulation of two-dimensional perfectly conducting cylinders illuminated by a TE-polarized Gaussian plane wave. The numerical results by the new scheme employing 2D Green's function and calculating time convolutions, differentials and integrals analytically are compared with the results from the TD-MoM technique using 3D time domain Green's function of free space [17] and the technique using 2D Green's function and calculation of temporal convolutions, differentials and integrals numerically [3], demonstrating its accuracy and efficiency. In [3, 17], the time-step size is chosen based on Courant's stability condition, but in the proposed technique the time-step size is selected according to the causality rule, therefore the greater time step sizes are used.

The unintended growing late-time oscillations are originated from the error of space-time discretization. However, the remarkable efficiency of the proposed TD-MoM formulation arises mainly from the analytical calculation of the time convolution integrals and the spatial integrals appearing in the TD-EFIE. Effect of choosing various temporal basis functions as a key factor to increasing stability and convergence of the TD-MoM solution is investigated. It is observed that by employing triangular and quadratic Lagrange TBFs, the stable region is vastly extended. But using shifted quadratic B-Spline function as a smooth causal temporal basis function, the instability is occurred earlier than expected because of interpolation errors and shifting in time.

APPENDIX A.

As noted in Section 2, all time convolutions, time differentials and time integrals in (13) to (15) can be calculated analytically. For instance, the time convolutions using the triangular TBF (6b) has been given as follows.

$$\frac{\partial}{\partial t} g_0(t) * G\left(\boldsymbol{\rho}, t; \boldsymbol{\rho}'\right)$$

$$= \frac{1}{2\pi\Delta t} \times \begin{cases} 0 & t - R/c < -\Delta t \\ \ln\left(\frac{t+\Delta t+\sqrt{(t+\Delta t)^2-(R/c)^2}}{(R/c)}\right) & -\Delta t \le t - R/c < 0 \\ \ln\left(\frac{t+\Delta t+\sqrt{(t+\Delta t)^2-(R/c)^2}}{(R/c)}\right) - 2\ln\left(\frac{t+\sqrt{t^2-(R/c)^2}}{(R/c)}\right) & 0 \le t - R/c < \Delta t \\ \ln\left(t+\Delta t+\sqrt{(t+\Delta t)^2-(R/c)^2}\right) - 2\ln\left(t+\sqrt{t^2-(R/c)^2}\right) & \\ \quad + \ln\left(t-\Delta t+\sqrt{(t-\Delta t)^2-(R/c)^2}\right) & t - R/c > \Delta t \end{cases} \quad \text{(A1)}$$

$$
\begin{aligned}
&G_0(t) * G(\boldsymbol{\rho}, t; \boldsymbol{\rho}') \\
&= \frac{1}{8\pi\Delta t} \times \begin{cases}
0, & t - R/c < -\Delta t \\
\left[2\left(t+\Delta t\right)^2 + \left(R/c\right)^2\right] \ln\left(\frac{t+\Delta t+\sqrt{\left(t+\Delta t\right)^2-\left(R/c\right)^2}}{\left(R/c\right)}\right) & \\
-3\left(t+\Delta t\right)\sqrt{\left(t+\Delta t\right)^2-\left(R/c\right)^2}, & -\Delta t \le t - R/c < 0 \\
\left\{\begin{array}{l}
\left[2\left(t+\Delta t\right)^2 + \left(R/c\right)^2\right] \ln\left(\frac{t+\Delta t+\sqrt{\left(t+\Delta t\right)^2-\left(R/c\right)^2}}{\left(R/c\right)}\right) \\
-\left(4t^2 + 2\left(R/c\right)^2\right) \ln\left(\frac{t+\sqrt{t^2-\left(R/c\right)^2}}{\left(R/c\right)}\right) \\
-3\left(t+\Delta t\right)\sqrt{\left(t+\Delta t\right)^2-\left(R/c\right)^2} + 6t\sqrt{t^2-\left(R/c\right)^2}
\end{array}\right\}, & 0 \le t - R/c < \Delta t \\
\left\{\begin{array}{l}
\left[2\left(t+\Delta t\right)^2 + \left(R/c\right)^2\right] \ln\left(\frac{t+\Delta t+\sqrt{\left(t+\Delta t\right)^2-\left(R/c\right)^2}}{\left(R/c\right)}\right) \\
-\left(4t^2 + 2\left(R/c\right)^2\right) \ln\left(\frac{t+\sqrt{t^2-\left(R/c\right)^2}}{\left(R/c\right)}\right) \\
+\left[2\left(t-\Delta t\right)^2 + \left(R/c\right)^2\right] \ln\left(\frac{t-\Delta t+\sqrt{\left(t-\Delta t\right)^2-\left(R/c\right)^2}}{\left(R/c\right)}\right) \\
-3\left(t+\Delta t\right)\sqrt{\left(t+\Delta t\right)^2-\left(R/c\right)^2} \\
+6t\sqrt{t^2-\left(R/c\right)^2} - 3\left(t-\Delta t\right)\sqrt{\left(t-\Delta t\right)^2-\left(R/c\right)^2}
\end{array}\right\}, & t - R/c > \Delta t,
\end{cases}
\end{aligned} \tag{A2}
$$

APPENDIX B.

In calculation of the propagation matrix $[\Phi^0]$ the self-coupling and near coupling elements have logarithmic singularity. With singularity extraction methods introduced in Section 3, the elements of $\varphi^0_{m,m}$ $\varphi^0_{m,(m+1)}$ and $\varphi^0_{(m+1),m}$ can be calculated as follow. With first-order approximation, the diagonal and near diagonal elements are:

$$\varphi^0_{m,m} = \frac{\mu_0(\Delta\tau_m)^2}{2\pi\Delta t}\left[\ln\left(\frac{4c\Delta t}{\Delta\tau_m}\right)+1\right] + \frac{2\mu_0 c^2\Delta t}{8\pi}\left[2\ln\left(\frac{4c\Delta t}{\Delta\tau_m}\right)-1\right], \quad m = 1, 2, \ldots, N_s \tag{B1}$$

$$\varphi^0_{m,(m+1)} = \varphi^0_{(m+1),m} = -\frac{\mu_0 c^2\Delta t}{8\pi}\left[2\ln(\frac{4c\Delta t}{\Delta\tau_m})-1\right], \quad m = 1, 2, \ldots, N_s - 1 \tag{B2}$$

and with second-order approximation, we have:

$$\varphi^0_{m,m} = \frac{\mu_0(\Delta\tau_m)^2}{2\pi\Delta t}\left[\ln\left(\frac{4c\Delta t}{\Delta\tau_m}\right)+\frac{3}{2}\right] + \frac{2\mu_0 c^2\Delta t}{8\pi}2\ln\left(\frac{4c\Delta t}{\Delta\tau_m}\right), \quad m = 1, 2, \ldots, N_s \tag{B3}$$

$$\varphi^0_{m,(m+1)} = \varphi^0_{(m+1),m} = -\frac{\mu_0 c^2\Delta t}{8\pi}2\ln\left(\frac{4c\Delta t}{\Delta\tau_m}\right), \quad m = 1, 2, \ldots, N_s - 1 \tag{B4}$$

REFERENCES

1. Hu, J. L. and C. H. Chan, "Improved temporal basis function for time domain electric field integral equation method," *Electronics Letters*, Vol. 35, No. 11, 883–885, 1999.
2. Zhang, G. H., M. Y. Xia, and X. M. Jiang, " Transient analysis of wire structures using time domain integral equation method with exact matrix elements," *Progress In Electromagnetics Research*, Vol. 92, 281–298, 2009.

3. Bennett, C. L. and W. L. Weeks, "Transient scattering from conducting cylinders," *IEEE Trans. Antennas Propagat.*, Vol. 18, No. 5, 627–633, 1970.
4. Rao, S. M., D. A. Vechinski, and T. K. Sarkar, "Transient scattering by conducting cylinders — Implicit solution for the transverse electric case," *Microwave and Opt. Tech. Lett.*, Vol. 21, No. 2, 129–134, 1999.
5. Geranmayeh, A., W. Ackermann, and T. Weiland, "Temporal discretization choices for stable boundary element method in electromagnetic scattering problems," *Applied Numerical Mathematics*, Vol. 59, No. 11, 2751–2773, 2009.
6. Rynne, B. P. and P. D. Smith, "Stability of time marching algorithms for the electric field integral equation," *Journal of Electromagnetic Waves and Applications*, Vol. 4, No. 12, 1181–1205, Dec. 1990.
7. Jung, B. H., Y.-S. Chung, and T. K. Sarkar, "Time domain EFIE, MFIE, and CFIE formulations using Laguerre polynomials as temporal basis functions for the analysis of transient scattering from arbitrary shaped conducting structures," *Progress In Electromagnetics Research*, Vol. 39, 1–45, 2003.
8. Ding, J., C. Gu, Z. Li, and Z. Niu, "Analysis of transient electromagnetic scattering using time domain fast dipole method," *Progress In Electromagnetics Research*, Vol. 136, 543–559, 2013.
9. Ding, J., L. Yu, W. Xu, C. Gu, and Z. Li, "Analysis of transient electromagnetic scattering using the multilevel dipole method," *Progress In Electromagnetics Research*, Vol. 140, 401–413, 2013.
10. Qin, S.-T., S.-X. Gong, R. Wang, and L.-X. Guo, "A TDIE/TDPO hybrid method for the analysis of TM transient scattering from two dimensional combinative conducting cylinders," *Progress In Electromagnetics Research*, Vol. 102, 181–195, 2010.
11. Geranmayeh, A., W. Ackermann, and T. Weiland, "Proper combination of integrators and interpolators for stable marching-on-in time schemes," *Proc. 10th Int. Conf. on Electromagnetics in Advance Applications (ICEAA' 07)*, 948–951, Torino, Italy, 2007.
12. Firouzeh, Z. H., R. Moini, S. H. H. Sadeghi, R. Faraji-Dana, and G. A. E. Vandenbosch, "A new robust technique for transient analysis of conducting cylinders — TM case," *5th European Conference on Antennas and Propagation, EuCAP 2011*, 1353–1356, Rome, Italy, Apr. 11–15, 2011.
13. Wang, P., M. Y. Xia, J. M. Jin, and L. Z. Zhou, "Time domain integral equation solvers using quadratic B-Spline temporal basis functions," *Microwave and Optical Technology Letters*, Vol. 49, No. 5, 1154–1159, 2007.
14. Glisson, A. W. and D. R. Wilton, "Simple and efficient numerical methods for problems of electromagnetic radiation and scattering from surfaces," *IEEE Trans. Antennas Propagat.*, Vol. 28, No. 5, 593–603, 1998.
15. Manara, G., A. Monorchio, and R. Reggiannini, "A space-time discretization criterion for a stable time-marching solution of the electric field integral equation," *IEEE Trans. Antennas Propagat.*, Vol. 45, No. 3, 527–532, 1997.
16. Dwight, H. B., *Tables of Integrals and Other Mathematical Data*, 3rd Edition, The Macmillan Company, 1957.
17. Rao, S. M., *Time Domain Electromagnetics*, Academic Press, New York, 1999.
18. Geranmayeh, A., W. Ackermann, and T. Weiland, "Survey of temporal basis functions for integral equation methods," *Proc. 7th IEEE Workshop on Computational Electromagnetics in Time-Domain, CEM-TD' 07*, Vol. 533, 1–4, Perugia, Italy, 2007.